The ground and the first excited states of an electron in a multidimensional polar semiconductor quantum dot: an all-coupling variational approach

1999 J. Phys.: Condens. Matter 11 2071

(http://iopscience.iop.org/0953-8984/11/9/005)

J. Phys.: Condens. Matter **11** (1999) 2071–2085. Printed in the UK PII: S0953-8984(99)93035-7

The ground and the first excited states of an electron in a multidimensional polar semiconductor quantum dot: an all-coupling variational approach

Soma Mukhopadhyay and Ashok Chatterjee
School of Physics, University of Hyderabad, Central University PO, Hyderabad 500 046, India

Received 3 April 1998, in final form 14 September 1998

Abstract. A variational calculation is performed to obtain the polaronic corrections to the ground and the first-excited-state energies of an electron in a parabolic quantum dot of a polar semiconductor for the entire range of the electron–phonon coupling constant and the confinement length. The number of virtual phonons, the size of the polaron and the polarization potential in the polaron ground state are also calculated. The theory is applied to both two- and three-dimensional GaAs quantum dots and it is shown that both the ground and the first-excited-state polaronic corrections in these dots can be considerably large if the dot sizes are of the order a few nanometres.

1. Introduction

The study of low dimensional systems has undergone a renaissance with the advent of modern fabrication techniques such as molecular beam epitaxy, nanolithographic and etching techniques and selective ion implantation. With the development of these techniques it is now possible to fabricate ultrasmall semiconductor structures with quantum confinement in all the spatial directions [1]. These structures are typically of the order of a few nanometres in size resembling giant artificial atoms and are commonly referred to as zero-dimensional objects or more technically as quantum dots (see [2] for a review). Because of the zero dimensionality quantum dots have fully quantized energy spectra and exhibit many new physical effects [3] such as optical and electronic transport characteristics which are quite different from those encountered in the case of their bulk counterparts. The quantum dot structures can be realized in both the two and three dimensions and can be fabricated in different shapes and sizes. Because of this design flexibility and the novel physical properties, quantum dots have tremendous potentiality in finding application in semiconductor-based micro-electronic device technology, for example in ultrafast computers. Consequently, a number of theoretical and experimental investigations [4] have lately gone into understanding and exploring various physical properties of these systems, among them the electronic properties being of particular interest.

The electron–phonon interaction should play an important role in determining the transport and other properties of quantum dots and has therefore been extensively studied [5] in these materials both theoretically and experimentally. Recently a number of authors [6–8] have also investigated the polaronic effects in quantum dots. Most of these calculations were however performed in the weak electron–phonon coupling regime. We have performed a path-integral variational calculation [7] for the polaron ground state (GS) self energy in a harmonic quantum

0953-8984/99/092071+15$19.50

dot for the entire range of the electron–phonon coupling strength. Sahoo [8] has also presented a variational calculation for the GS polaronic properties of a harmonic dot. His calculation is based on the Lee–Low–Pines–Huybrechts (LLPH) approach. However his assertion that the total momentum of the system commutes with the Hamiltonian and is thus a constant of motion is not correct and therefore the idea of minimizing the functional $\langle\tilde{\Psi}|\tilde{H} - \vec{u}\tilde{\vec{P}}|\Psi\rangle$ (equation (3) of [8]) in this problem conceived by him is erroneous. Furthermore, the electronic wavefunction (equation (9) of [8]) chosen by Sahoo is just the ground state wavefunction of the confining potential and does not contain any variational parameters which implies that his calculation is not valid for all values of the electron–phonon coupling constant and the confinement length. His effective mass calculation is also not very meaningful in the strong confinement regime where the quantum dot enhancements of the polaronic properties are significant. In the present paper we purport to present an all-coupling LLPH calculation for the GS polaron self-energy, the number of virtual phonons in the polaron, the size of the polaron and the GS polarization potential of a polaron in a symmetric parabolic quantum dot for the entire range of the confinement length. Comparison of the LLPH results with the corresponding Feynman–Haken path-integral results [7] shows that the LLPH results are quite accurate. The LLPH method however has one palpable advantage over the path-integral method in that it can be applied to the excited states (ESs). We also report in the present paper our LLPH results for the first excited state.

For the sake of mathematical simplicity we neglect the size quantization of phonons and treat the relevant phonon modes within the framework of the Fröhlich model [9]. This approach may not be rigorously valid if the confinement length is reduced to a very small value, but may still serve as a good enough approximation to capture some of the most important and interesting features of the electron–phonon interaction effects in quantum dots. We shall make an N-dimensional (ND) formulation and obtain results for both 2D and 3D dots as special cases. In our model, a quantum dot embedded in a 3D material with the motion of the dot electron confined in all the three spatial directions will be called a 3D quantum dot, while that embedded in a purely two-dimensional (zero-thickness) system with the electron's motion confined in the two available spatial directions will be referred to as a 2D quantum dot.

2. The model Hamiltonian

The system under study consists of an electron interacting with the longitudinal optical (LO) phonons of an ND polar semiconductor quantum dot. Theoretically one can simulate the ND quantum dot geometry approximately by considering the electron's motion in an N-dimensional box. This model is however not very realistic since the force experienced by the electron within the dot is not really zero. A number of recent investigations [10] on the other hand have indeed suggested that the confining potential seen by an electron in a quantum dot is nearly parabolic. We shall therefore use the parabolic potential model in the present work. The Hamiltonian for an electron moving in an ND parabolic quantum dot and interacting with LO phonons of the system can be written as

$$H' = -\frac{\hbar^2}{2m}\nabla^2_{\vec{r}'} + \frac{1}{2}m\sum_i \omega^2_{hi}x_i'^2 + \hbar\omega_{LO}\sum_{\vec{q}'} b^\dagger_{\vec{q}'}b_{\vec{q}'} + \sum_{\vec{q}'}[\xi'_{\vec{q}'}\,\mathrm{e}^{-\mathrm{i}\vec{q}'\cdot\vec{r}'}b^\dagger_{\vec{q}'} + \mathrm{HC}] \tag{1}$$

where all vectors are ND, $\vec{r}'(x_i', x_2', \ldots, x_N')$ is the position vector of the electron and m is its Bloch effective mass, ω_{hi} is the frequency of the confining potential in the ith direction, ω_{LO} is the LO phonon frequency which is assumed to be dispersionless, $b^\dagger_{\vec{q}'}$ ($b_{q'}$) is the creation (annihilation) operator for an LO phonon of wavevector $\vec{q}'$ and $\xi'_{q'}$ is the electron–phonon

interaction coefficient. We shall use the Feynman units in which the energy is scaled by $\overline{h}\omega_{LO}$, length by r_0 where $r_0 = q_0^{-1}$, q_0 being an inverse length defined by $\overline{h}^2 q_0^2/m = \overline{h}\omega_{LO}$, volume by r_0^N and wavevectors by q_0. Such scalings are equivalent to putting $\overline{h} = m = \omega_{LO} = 1$. In these units the Hamiltonian (1) reads

$$H = -\frac{1}{2}\nabla_{\vec{r}}^2 + \frac{1}{2}\sum_i \omega_i^2 x_i^2 + \sum_{\vec{q}} b_q^\dagger b_{\vec{q}} + \sum_{\vec{q}} (\xi_q \, \mathrm{e}^{-\mathrm{i}\vec{q}\cdot\vec{r}} b_{\vec{q}}^\dagger + \mathrm{HC}) \tag{2}$$

where $r^2 = \sum_{i=1}^N x_i^2$, $x_i = x_i'/r_0$, $\vec{q} = \vec{q}/q_0$, $\omega_i = \omega_{hi}/\omega_{LO}$ and ξ_q is given by [11]

$$|\xi_q|^2 = \frac{\Gamma\left(\frac{N-1}{2}\right) 2^{N-\frac{3}{2}} \pi^{\left(\frac{N-1}{2}\right)}}{V_N q^{N-1}} \alpha \tag{3}$$

where V_N is the volume of the ND dot and α is the dimensionless electron–phonon coupling constant.

3. Formulation

In the LLPH method [12, 13] the first LLP transformation is modified as

$$U_1 = \exp\left[-\mathrm{i}a \sum_{\vec{q}} \vec{q}\cdot\vec{r} b_{\vec{q}}^\dagger b_{\vec{q}} \right] \tag{4}$$

where a is a variational parameter. Then after the second LLP transformation [14]

$$U_2 = \exp\left[\sum_{\vec{q}} (f_{\vec{q}} b_{\vec{q}}^\dagger - f_{\vec{q}}^* b_{\vec{q}}) \right] \tag{5}$$

the Hamiltonian (2) becomes

$$\begin{aligned}\tilde{H} = U_2^{-1}U_1^{-1}HU_1U_2 = {} & \frac{\hat{\vec{p}}^2}{2} + \sum_{\vec{q}} \left(1 + \frac{a^2q^2}{2} - a\vec{p}\cdot\vec{q}\right)(b_{\vec{q}}^\dagger + f_q^*)(b_{\vec{q}} + f_{\vec{q}}) \\ & + \frac{1}{2}\sum_i \omega_i^2 x_i^2 + \sum_{\vec{q}} [\xi_q \, \mathrm{e}^{-\mathrm{i}(1-a)\vec{q}\cdot\vec{r}} (b_{\vec{q}}^\dagger + f_{\vec{q}}^*) + \mathrm{HC}] \\ & + \frac{a^2}{2}\sum_{\vec{q},\vec{q}} \vec{q}\cdot\vec{q}'(b_{\vec{q}}^\dagger + f_{\vec{q}}^*)(b_{\vec{q}'}^\dagger + f_{\vec{q}'}^*)(b_{\vec{q}} + f_{\vec{q}})(b_{\vec{q}'} + f_{\vec{q}'})\end{aligned} \tag{6}$$

where $\hat{\vec{p}}$ is the electron momentum and the function $f_{\vec{q}}$ is to be obtained variationally. When $a = 1$ this modified procedure reduces to the LLP method, which should provide a good description in the extended state limit, while for $a = 0$ this approach is equivalent to the Landau–Pakar method [13], which is valid in the adiabatic limit and will be a useful approach in the localized state limit. Thus treating a as a variational parameter ($0 < a < 1$) one can have a consistent theory encompassing the entire parameter space. The variational energy is now written as

$$E = \langle\Phi|\langle 0|\tilde{H}|0\rangle|\Phi\rangle \tag{7}$$

where $\Phi(\vec{r})$ is the electronic function to be chosen variationally and $|0\rangle$ is the unperturbed zero-phonon state. We are interested in this work in a symmetric quantum dot and therefore we assume

$$\sum_{\vec{q}} \vec{q}|f_{\vec{q}}|^2 = 0 \tag{8}$$

and the variational energy then simplifies to

$$E = -\frac{1}{2}\langle\Phi|\nabla^2|\Phi\rangle + \left[\sum_{\vec{q}}\left(1+\frac{a^2q^2}{2}\right)|f_q|^2\right]\left[\frac{1}{2}\sum_i \omega_i^2\langle\Phi|x_i^2|\Phi\rangle\right] + \sum_{\vec{q}}(\xi_q f_q^* \rho_{\vec{q}}^* + \text{HC}) \quad (9)$$

where

$$\rho_{\vec{q}} = \langle\Phi|e^{i(1-a)\vec{q}\cdot\vec{r}}|\Phi\rangle. \quad (10)$$

Minimizing E with respect to f_q^* now yields

$$f_q = -\frac{\xi_q \rho_{\vec{q}}^*}{\left(1+\frac{a^2q^2}{2}\right)} \quad (11)$$

and thus equation (9) reduces to

$$E = -\frac{1}{2}\langle\Phi|\nabla^2|\Phi\rangle + \frac{1}{2}\sum_i \omega_i^2\langle\Phi|x_i^2|\Phi\rangle - \sum_{\vec{q}}\frac{|\xi_q|^2|\rho_{\vec{q}}|^2}{\left(1+\frac{a^2q^2}{2}\right)}. \quad (12)$$

The average number of phonons ($\mathcal{N}$) in the polaron may be defined as

$$\mathcal{N} = \langle\Psi|b_{\vec{q}}^\dagger b_{\vec{q}}|\Psi\rangle \quad (13)$$

and the size of the polaron ($\mathcal{R}$) may be defined as

$$\mathcal{R} = \langle\Psi|r|\Psi\rangle \quad (14)$$

where

$$|\Psi\rangle = U_1U_2|0\rangle|\Phi\rangle. \quad (15)$$

We obtain

$$\mathcal{N} = \sum_{\vec{q}}\frac{|\xi_q|^2|\rho_{\vec{q}}|^2}{\left(1+\frac{a^2q^2}{2}\right)^2} \quad (16)$$

and

$$\mathcal{R} = \langle\Phi|r|\Phi\rangle. \quad (17)$$

Another interesting quantity is the polarization potential which can be defined as

$$V(\vec{r}') = \langle\Psi|v(\vec{r}-\vec{r}')|\Psi\rangle \quad (18)$$

where

$$v(\vec{r}) = -\frac{1}{e}\sum_{\vec{q}}(\xi_q\, e^{-i\vec{q}\cdot\vec{r}} b_{\vec{q}}^\dagger + \text{HC}). \quad (19)$$

We obtain

$$-eV(\vec{r}) = -2\sum_{\vec{q}}\frac{|\xi_q|^2|\rho_{\vec{q}}|^2}{\left(1+\frac{a^2q^2}{2}\right)}\cos(\vec{q}\cdot\vec{r}'). \quad (20)$$

4. The ground state

So far we have not specified the form of the electronic function for which we now make the harmonic oscillator approximation, i.e. we choose

$$\Phi(\vec{r}) = \prod_{i=1}^{N} \phi(x_i) \tag{21}$$

with

$$\phi(x_i) = \frac{\sqrt{\mu_i}}{\pi^{1/4}} \, \mathrm{e}^{-\mu_i^2 x_i^2/2} \tag{22}$$

where μ_i are variational parameters. We then obtain

$$\rho_{\vec{q}} = \exp\left[-\sum_{i=1}^{N} \frac{(1-a)^2}{4\mu_i^2} q_i^2 \right] \tag{23}$$

and thus the GS energy, the mean number of phonons in the GS polaron, the polaron size and the GS polarization potential assume the following expressions:

$$E_{GS} = \frac{1}{4}\sum_i \mu_i^2 + \frac{1}{4}\sum_i \frac{\omega_i^2}{\mu_i^2} - \frac{\Gamma\left(\frac{N-1}{2}\right)\alpha}{2\sqrt{2}\pi^{\frac{N+1}{2}}} \int \frac{\mathrm{d}\vec{q}\, \mathrm{e}^{-\sum_i \frac{(1-a)^2}{2\mu_i^2} q_i^2}}{q^{N-1}\left(1+\frac{a^2q^2}{2}\right)} \tag{24}$$

$$\mathcal{N}_{GS} = \frac{\Gamma\left(\frac{N-1}{2}\right)\alpha}{2\sqrt{2}\pi^{\frac{N+1}{2}}} \int \frac{\mathrm{d}\vec{q}\, \mathrm{e}^{-\sum_i \frac{(1-a)^2}{2\mu_i^2} q_i^2}}{q^{N-1}\left(1+\frac{a^2q^2}{2}\right)^2} \tag{25}$$

$$\mathcal{R}_{GS} = \frac{\mu_1\mu_2\ldots\mu_N}{\pi^{N/2}} \int \mathrm{d}\vec{r} r \, \mathrm{e}^{-\sum_i \mu_i^2 x^2} \tag{26}$$

$$-eV_{GS}(\vec{r}) = -\frac{\Gamma\left(\frac{N-1}{2}\right)\alpha}{\sqrt{2}\pi^{\frac{N+1}{2}}} \int \frac{\mathrm{d}\vec{q}}{q^{N-1}} \frac{\mathrm{e}^{-\sum_i \frac{(1-a)^2}{2\mu_i^2} q_i^2} \cos(\vec{q}\vec{r})}{\left(1+\frac{a^2q^2}{2}\right)}. \tag{27}$$

We are interested in a symmetric quantum dot for which, we have $\omega_1 = \omega_2 = \cdots = \omega_N = \omega$ and therefore we can take $\mu_1 = \mu_2 = \cdots = \mu_N = \mu$. Equations (24)–(27) then read

$$E_{GS} = \frac{N}{4}\mu^2 + \frac{N}{4l^4\mu^2} - \frac{\sqrt{\pi}\alpha}{2}\frac{\Gamma\left(\frac{N-1}{2}\right)}{\Gamma(N/2)}(1+t\mu)\,\mathrm{e}^{t^2}\mathrm{erfc}(t) \tag{28}$$

$$\mathcal{N}_{GS} = \frac{\alpha}{\sqrt{2\pi}}\frac{\Gamma\left(\frac{N-1}{2}\right)}{\Gamma(N/2)} \int_0^\infty \mathrm{d}q \frac{\mathrm{e}^{-\frac{(1-a)^2}{2\mu^2}q^2}}{\left(1+\frac{a^2q^2}{2}\right)^2} \tag{29}$$

$$\mathcal{R}_{GS} = \frac{\Gamma\left(\frac{N+1}{2}\right)}{\Gamma(N/2)}\frac{1}{\mu} \tag{30}$$

$$-eV_{GS}(\vec{r}) = -\frac{\alpha 2^{\frac{N-1}{2}}\Gamma\left(\frac{N-1}{2}\right)}{\sqrt{\pi}} \frac{1}{r^{\frac{N}{2}-1}} \int \mathrm{d}q \frac{\mathrm{e}^{-\frac{(1-a)^2}{2\mu^2}q^2}}{q^{\frac{N}{2}-1}\left(1+\frac{a^2q^2}{2}\right)} J_{\frac{N}{2}-1}(qr). \tag{31}$$

In (28), l is the dimensionless confinement length given by $l = l_0/r_0 = \frac{1}{\sqrt{\omega}}$, where $l_0 = (\hbar/m\omega_h)^{1/2}$ and $t = (\frac{1-a}{a\mu})$ is to be treated as a new variational parameter instead of

a. Variation of (28) with respect to μ and t gives

$$\mu^4 - \left[\frac{\alpha\sqrt{\pi}}{3}\frac{\Gamma\left(\frac{N-1}{2}\right)}{\Gamma(N/2)} t\, \mathrm{e}^{t^2}\mathrm{erfc}(t)\right]\mu^3 - \frac{1}{l^4} = 0 \tag{32}$$

$$2(1+\mu t) + \sqrt{\pi}\,\mathrm{e}^{t^2}\mathrm{erfc}(t)(\mu + 2\sqrt{\pi}(1+\mu t)) = 0 \tag{33}$$

which have to be solved numerically. However in the limiting cases it is possible to obtain analytical expressions.

4.1. Extended state limit

When the effective confinement length is large and the electron–phonon interaction is weak, the electron wavefunction will be of extended type and will be spread over many lattice points. Thus in this extended state limit, both ω and α are small and therefore we can take the limit, $t \to 0$. Using the limiting results

$$\mathrm{e}^{t^2}\mathrm{erfc}(t) = \mathrm{e}^{t^2} - \frac{2}{\sqrt{\pi}}\sum_{n=0}^{\infty}\frac{2^n}{(2n+1)!!}t^{2n+1} \underset{t\to 0}{\longrightarrow} 1 \tag{34}$$

$$t\,\mathrm{e}^{t^2}\mathrm{erfc}(t) \underset{t\to 0}{\longrightarrow} 0 \tag{35}$$

we then obtain

$$E_{GS} = \frac{N}{4}\mu^2 + \frac{N}{4\mu^2 l^4} - \frac{\sqrt{\pi}\alpha}{2}\frac{\Gamma\left(\frac{N-1}{2}\right)}{\Gamma(N/2)} \tag{36}$$

which on minimization with respect to μ gives

$$\mu^2 = \frac{1}{l^2}. \tag{37}$$

We thus obtain

$$E_{GS} = \frac{N}{2l^2} - \frac{\alpha\sqrt{\pi}}{2}\frac{\Gamma\left(\frac{N-1}{2}\right)}{\Gamma(N/2)} \tag{38}$$

$$\mathcal{N}_{GS} = \frac{\alpha\sqrt{\pi}}{4}\frac{\Gamma\left(\frac{N-1}{2}\right)}{\Gamma(N/2)} \tag{39}$$

$$\mathcal{R}_{GS} = \frac{\Gamma\left(\frac{N+1}{2}\right)}{\Gamma(N/2)} l \tag{40}$$

$$-eV_{GS}(\vec{r}) = -\frac{\alpha 2^{\frac{N-1}{2}}\Gamma\left(\frac{N-1}{2}\right)}{\sqrt{\pi} r^{\frac{N}{2}-1}}\int_0 \frac{J_{\frac{N}{2}-1}(qr)\,\mathrm{d}q}{q^{\frac{N}{2}-1}\left(1+\frac{q^2}{2}\right)}. \tag{41}$$

It is interesting to note that in the extended state limit the average number of phonons and the polarization potential are independent of l and depend only on α linearly, while the polaron size decreases with decreasing l and is independent of the electron–phonon coupling constant α.

4.2. Localized state limit

If both the confining potential and the electron–phonon interaction are strong or one of them is strong, the electron wavefunction will be of localized type. In this case, $t \to \infty$. We therefore use the asymptotic relation

$$\sqrt{\pi}t\,\mathrm{e}^{t^2}\mathrm{erfc}(t) \underset{t\to\infty}{\sim} 1 + \sum_{m=1}^{\infty}(-1)^m\frac{1.3\ldots(2m-1)}{(2t^2)^m} \tag{42}$$

to obtain

$$E_{GS} = \frac{N}{4}\mu^2 + \frac{N}{4\mu^2 l^4} - \frac{\alpha}{2}\frac{\Gamma\left(\frac{N-1}{2}\right)}{\Gamma(N/2)}\mu \tag{43}$$

$$\mathcal{N}_{GS} = \frac{\alpha}{2}\frac{\Gamma\left(\frac{N-1}{2}\right)}{\Gamma(N/2)}\mu \tag{44}$$

$$\mathcal{R}_{GS} = \frac{\Gamma\left(\frac{N+1}{2}\right)}{\Gamma(N/2)}\frac{1}{\mu} \tag{45}$$

$$-eV_{GS}(\vec{r}) = -\alpha\mu\frac{\Gamma\left(\frac{N-1}{2}\right)}{\Gamma(N/2)}\,{}_1F_1\left(\frac{1}{2}, \frac{N}{2}; -\frac{\mu^2 r^2}{2}\right). \tag{46}$$

Minimization of E_{GS} with respect to μ leads to the equation

$$\mu^4 - \left\{\frac{\alpha}{N}\frac{\Gamma\left(\frac{N-1}{2}\right)}{\Gamma(N/2)}\right\}\mu^3 - \frac{1}{l^4} = 0 \tag{47}$$

which has to be solved to obtain μ. In the case of strong electron–phonon coupling and weak confinement equation (47) can be approximately solved to give

$$\mu = \frac{\alpha}{N}\frac{\Gamma\left(\frac{N-1}{2}\right)}{\Gamma(N/2)} \tag{48}$$

so that equations (43)–(46) reduce to

$$E_{GS} = -\frac{\alpha^2}{4N}\left\{\frac{\Gamma\left(\frac{N-1}{2}\right)}{\Gamma(N/2)}\right\}^2 + \frac{N^3}{4l^4\alpha^2}\left\{\frac{\Gamma(N/2)}{\Gamma\left(\frac{N-1}{2}\right)}\right\}^2 \tag{49}$$

$$\mathcal{N}_{GS} = \frac{\alpha^2}{2N}\left\{\frac{\Gamma\left(\frac{N-1}{2}\right)}{\Gamma(N/2)}\right\}^2 \tag{50}$$

$$\mathcal{R}_{GS} = \frac{N}{\alpha}\frac{\Gamma\left(\frac{N+1}{2}\right)}{\Gamma\left(\frac{N-1}{2}\right)} \tag{51}$$

$$-eV_{GS}(\vec{r}) = -\frac{\alpha^2}{N}\left\{\frac{\Gamma\left(\frac{N-1}{2}\right)}{\Gamma(N/2)}\right\}^2\,{}_1F_1\left(\frac{1}{2}, \frac{N}{2}; -\frac{\alpha^2}{N^2}\left\{\frac{\Gamma\left(\frac{N-1}{2}\right)}{\Gamma(N/2)}\right\}^2\frac{r^2}{2}\right). \tag{52}$$

In the opposite limit of strong confinement and weak electron–phonon coupling, the $\alpha\mu^3$ term in (47) can be neglected and we obtain

$$\mu^2 = \frac{1}{l^2} \tag{53}$$

so that equations (43)–(46) read

$$E_{GS} = \frac{N}{2l^2} - \frac{\alpha}{2}\frac{\Gamma\left(\frac{N-1}{2}\right)}{\Gamma(N/2)}\frac{1}{l} \tag{54}$$

$$\mathcal{N}_{GS} = \frac{\alpha}{2}\frac{\Gamma\left(\frac{N-1}{2}\right)}{\Gamma(N/2)}\frac{1}{l} \tag{55}$$

$$\mathcal{R}_{GS} = \frac{\Gamma\left(\frac{N+1}{2}\right)}{\Gamma(N/2)}l \tag{56}$$

$$-eV_{GS}(\vec{r}) = -\frac{\alpha}{l}\frac{\Gamma\left(\frac{N-1}{2}\right)}{\Gamma(N/2)}\,{}_1F_1\left(\frac{1}{2}, \frac{N}{2}; -\frac{r^2}{2l^2}\right). \tag{57}$$

Thus one can see that in the limit of strong confinement and weak electron–phonon coupling the average number of phonons and the polarization potential are functions of both α and l but the polaron size depends on l alone while in the case of strong electron–phonon coupling and weak confinement the average number of phonons, the polaron size and the polarization potential are all governed by the parameter α alone and do not depend on l at all.

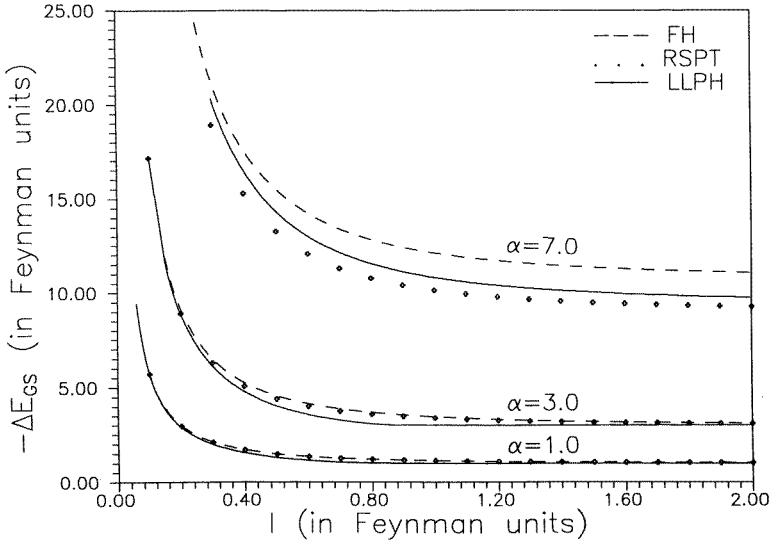

Figure 1. Polaronic corrections, $-\Delta E_{GS}$ (in Feynman units), to the GS energy of an electron in a parabolic quantum dot in 3D as a function of the confinement length (in Feynman units). The solid lines refer to the LLPH results while the dashed and the dotted curves correspond to the Feynman–Haken path-integral results and the RSPT results respectively.

4.3. Numerical results

As we have already pointed out, for arbitrary values of α and l, equations (32) and (33) have to be solved numerically. We define the GS polaronic correction (ΔE_{GS}) as

$$\Delta E_{GS} = E_{GS} - \frac{N}{2l^2} \tag{58}$$

which we obtain for both $N = 2$ and $N = 3$. In figure 1 we plot $-\Delta E_{GS}$ as a function of the dimensionless confinement length l for three values of α ($\alpha = 1, 3, 7$) for the 3D dot. In figure 2 we plot the corresponding results for the 2D dot. As expected, we find that the polaronic correction to the GS energy of a quantum dot electron becomes extremely large in both 2D and 3D when the dot sizes are made sufficiently small. With increasing confinement length the polaronic corrections however diminish in both 2D and 3D quantum dots. This decrease in the polaronic correction with increasing l is very rapid for small l, whereas if l exceeds a certain value the polaronic correction varies rather slowly with l, assuming asymptotically a constant value, essentially independent of the size of the dot. This is the usual bulk polaron limit. Furthermore, the quantum dot enhancement is larger in a 2D dot than in a 3D dot. To see the efficacy of the present variational method we compare in figures 1 and 2 the LLPH results with those obtained form Rayleigh–Schrödinger perturbation theory (RSPT) and the Feynman–Haken path-integral method. It is clear that the LLPH results are quite close to those obtained from the Feynman–Haken path-integral method which is known to yield very

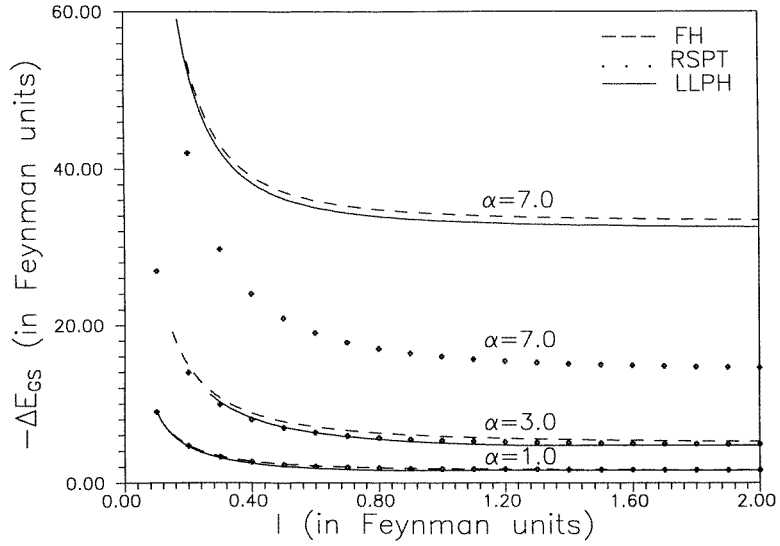

Figure 2. Polaronic corrections, $-\Delta E_{GS}$ (in Feynman units), to the GS energy of an electron in a parabolic quantum dot in 2D as a function of the confinement length l (in Feynman units). The solid lines refer to the LLPH results while the dashed and the dotted curves correspond to the Feynman–Haken path-integral results and the RSPT results respectively.

accurate results. Comparison of our results with those of Sahoo [8] (not shown here) shows that our results are much better for the entire range of the parameter values.

In figure 3 we plot the polarization potential for both 2D and 3D dots as a function of r for $\alpha = 3$ and for four values of l ($l = 0.03, 0.05, 1$ and 5). It is clear that the polarization potential is deeper in a 2D dot than in a 3D dot. Furthermore, as the confinement length decreases, the polarization potential becomes more and more deeper and is able to support lower polaronic GS levels.

5. The first excited state

For the first excited state which is N-fold degenerate we take the electronic function Φ for the symmetric quantum dot as

$$\Phi = \left(\frac{2\mu^{N+2}}{\pi^{N/2}}\right)^{1/2} x_N \, \mathrm{e}^{-\frac{1}{2}\mu^2 r^2}. \tag{59}$$

$\rho_{\vec{q}}$ is then given by

$$\rho_{\vec{q}} = \left(1 - \frac{(1-a)^2 q_N^2}{2\mu^2}\right) \mathrm{e}^{-(1-a)^2 q^2/4\mu^2} \tag{60}$$

where q_N is the Nth component of $\vec{q}$. The first excited state (ES) energy thus becomes

$$E_{GS} = \left(\frac{N+2}{4}\right)\mu^2 + \left(\frac{N+2}{4}\right)\frac{1}{\mu^2 l^4} - \frac{\alpha}{2\sqrt{2}\pi^{\frac{N+2}{2}}} \int \frac{\mathrm{d}\vec{q}\, \mathrm{e}^{-(1-a)^2 q^2/2\mu^2}}{q^{N-1}\left(1 + \frac{a^2 q^2}{2}\right)}$$
$$\times \left(1 - \frac{(1-a)^2 q_N^2}{2\mu^2}\right)^2 = \left(\frac{N+2}{4}\right)\mu^2 + \left(\frac{N+2}{4}\right)\frac{1}{\mu^2 l^4}$$

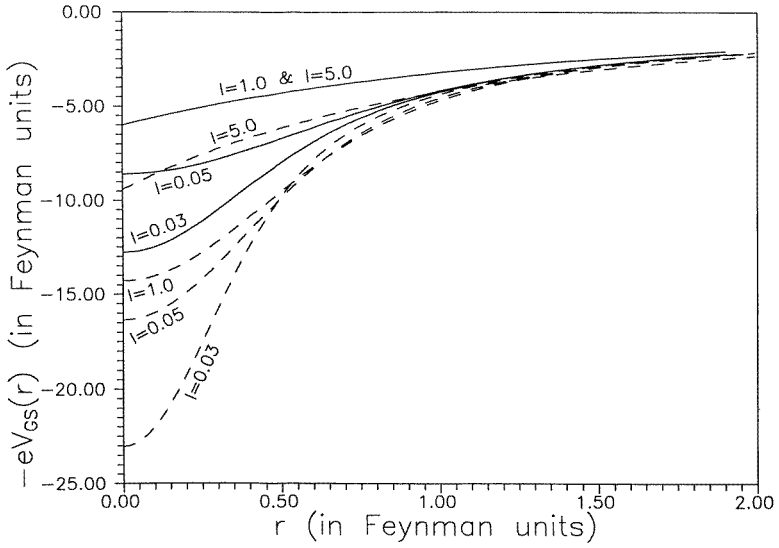

Figure 3. GS polarization potential energy, $-eV_{GS}(r)$ (in Feynman units), of an electron in 2D and 3D quantum dots as a function of r. The solid lines refer to the 3D quantum dots and the dashed curves correspond to the 2D dots.

$$-\frac{\alpha\Gamma\left(\frac{N-1}{2}\right)}{\sqrt{2\pi}\Gamma(N/2)}\int\frac{\mathrm{d}q\,\mathrm{e}^{-(1-a)^2q^2/2\mu^2}}{\left(1+\frac{a^2q^2}{2}\right)}\left\{1-\frac{(1-a)^2q^2}{N\mu^2}+\frac{3(1-a)^4q^4}{4N(N+2)\mu^4}\right\} \quad (61)$$

which has to be minimized numerically with respect to μ and a. Before discussing the numerical results we shall present the interesting limiting cases in which simple analytical results could be obtained.

5.1. Extended state limit ($a \to 1$)

In this limit, equation (61) becomes

$$E_{GS}=\left(\frac{N+2}{4}\right)\mu^2+\left(\frac{N+2}{4}\right)\frac{1}{\mu^2 l^4}-\frac{\alpha\sqrt{\pi}\Gamma\left(\frac{N-1}{2}\right)}{2\Gamma(N/2)}. \quad (62)$$

Minimization of (62) with respect to μ yields

$$\mu^2=\frac{1}{l^2} \quad (63)$$

and thus we obtain

$$E_{GS}=\left(\frac{N+2}{2}\right)\frac{1}{l^2}-\frac{\alpha\sqrt{\pi}\Gamma\left(\frac{N-1}{2}\right)}{2\Gamma(N/2)}. \quad (64)$$

5.2. Localized state limit

In the localized state limit we have $a = 0$ and therefore equation (61) becomes

$$E_{GS}=\left(\frac{N+2}{4}\right)\mu^2+\left(\frac{N+2}{4}\right)\frac{1}{\mu^2 l^4}-\frac{(2N+1)^2\Gamma\left(\frac{N-1}{2}\right)}{16(N+2)\Gamma\left(\frac{N}{2}+1\right)}\mu\alpha. \quad (65)$$

Minimization of (65) with respect to μ gives

$$\left(\frac{N+2}{2}\right)\mu^4 - \left(\frac{N+2}{2}\right)\frac{1}{l^4} - \frac{(2N+1)^2\Gamma\left(\frac{N-1}{2}\right)}{16(N+2)\Gamma\left(\frac{N}{2}+1\right)}\alpha\mu^3 = 0. \tag{66}$$

In the limit of weak confinement and strong electron–phonon coupling we can neglect the second term of (66) and thus obtain

$$\mu = \frac{(2N+1)^2\Gamma\left(\frac{N-1}{2}\right)}{8(N+2)^2\Gamma\left(\frac{N}{2}+1\right)}\alpha \tag{67}$$

which yields

$$E_{GS} = -\frac{\left(N+\frac{1}{2}\right)^4}{16(N+2)^3}\left[\frac{\Gamma\left(\frac{N-1}{2}\right)}{\Gamma\left(\frac{N}{2}+1\right)}\right]^2\alpha^2 + \frac{(N+2)^5}{\left(N+\frac{1}{2}\right)^4}\left[\frac{\Gamma\left(\frac{N}{2}+1\right)}{\Gamma\left(\frac{N-1}{2}\right)}\right]^2\frac{1}{l^4\alpha^2} \tag{68}$$

which without the last term can be obtained by using the Landau–Pekar method with the Gaussian function as the trial electronic function. In the case of weak electron–phonon coupling and strong confinement we can neglect the $\alpha\mu^3$-term of (66) and thus obtain

$$\mu^2 = \frac{1}{l^2} \tag{69}$$

and

$$E_{ES} = \left(\frac{N+2}{2}\right)\frac{1}{l^2} - \frac{\left(N+\frac{1}{2}\right)}{4(N+2)}\frac{\Gamma\left(\frac{N-1}{2}\right)}{\Gamma\left(\frac{N}{2}+1\right)}\frac{\alpha}{1}. \tag{70}$$

5.3. Numerical results

We define the polaronic correction (ΔE_{ES}) in the first excited state as

$$\Delta E_{ES} = E_{ES} - \frac{(N+2)}{2l^2} \tag{71}$$

where E_{ES} is obtained from (61) by numerically minimizing it with respect to μ and a. We obtain ΔE_{ES} for both $N = 2$ and $N = 3$. In figure 4 we plot $-\Delta E_{ES}$ as a function of the dimensionless confinement length l for three values of α ($\alpha = 1, 5, 9$) for $N = 3$. For the sake of comparison we also plot in figure 4 the GS polaronic correction, $-\Delta E_{GS}$. It is clear that both the GS and the ES corrections become extremely large for small values of l. One can also see that for weak-coupling dots the polaronic corrections to the first ES are essentially same as that for the GS for large confinement length. However for small dots of the same material the ES corrections are found to be somewhat smaller than the GS corrections. For strong coupling quantum dots on the other hand we find that the polaronic corrections for the ES are always smaller than that for the GS no matter how large is the confinement length and in the case of small dots the difference ($\Delta E_{GS} - \Delta E_{ES}$) is of course quite significant. In figure 5 we plot $-\Delta E_{ES}$ for $N = 2$. The results are qualitatively same as those obtained for the 3D dots. Quantitatively however the polaronic enhancements are much larger in 2D dots than in 3D dots. We furthermore observe that the difference between the GS and the first ES polaronic corrections in the case of 2D dots can be considerably large even for moderate values of α and l.

We finally plot in figure 6 the ES polaronic correction, $-E_{ES}$, for both 2D and 3D GaAs quantum dots as a function of the confinement length l_0. For the sake of comparison we also plot the GS energy correction, $-\Delta E_{GS}$. The values of the material parameters used in the calculation have been taken from [15]. One can easily see that both the ground and the first

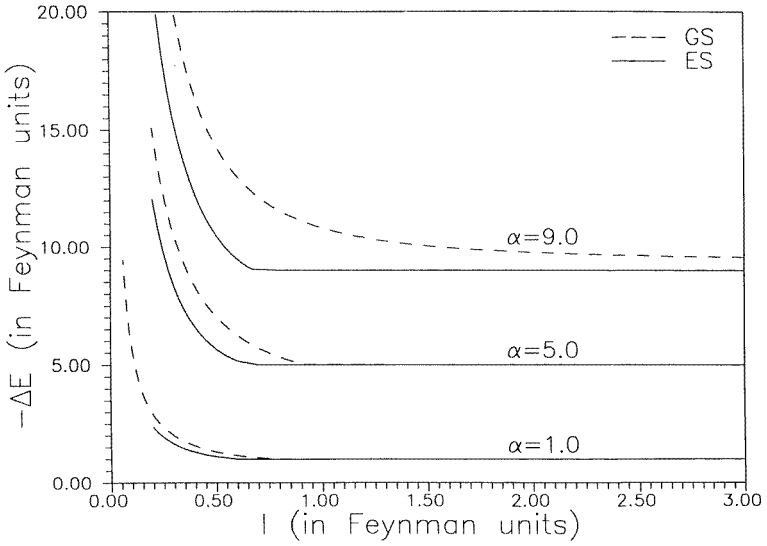

Figure 4. Polaronic corrections, $-\Delta E_{ES}$ (in Feynman units), to the ES energy of an electron in 3D quantum dots as a function of the confinement length l (in Feynman units). The GS energy corrections are also plotted for comparison.

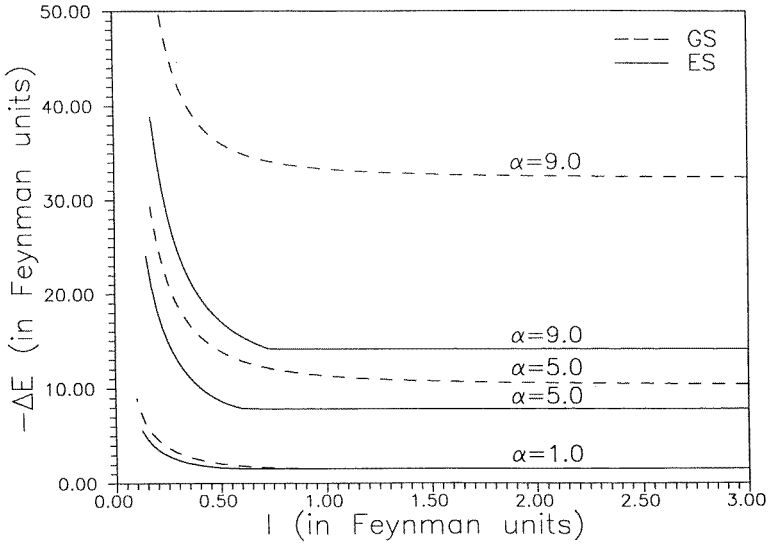

Figure 5. Polaronic corrections, $-\Delta E_{ES}$ (in Feynman units), to the ES energy of an electron in 2D quantum dots as a function of the confinement length l (in Feynman units). The GS energy corrections are also plotted for comparison.

excited state polaronic corrections can be considerably large for small GaAs quantum dots, the corrections being however larger in 2D dots than in the corresponding 3D ones. It is again interesting to note that the polaronic corrections ΔE_{GS} and ΔE_{ES} are essentially the same for large values of l in both 2D and 3D GaAs quantum dots, but below a certain value of l, which depends on the dimensionality of the dot, the difference $(\Delta E_{GS} - \Delta E_{ES})$ becomes non-

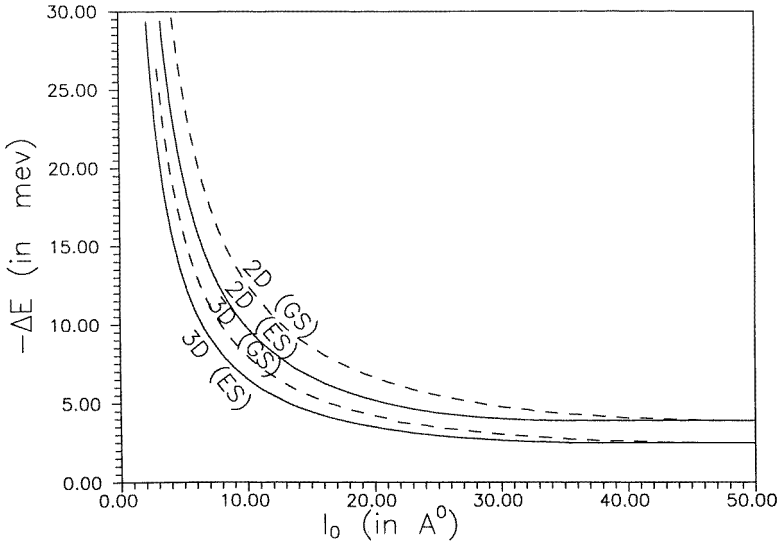

Figure 6. Polaronic corrections, $-\Delta E_{ES}$ (in meV), to the ES energy of an electron in 2D and 3D GaAs dots as a function of the confinement length, l_0 (in Å). The GS results are also plotted for comparison.

zero, ΔE_{GS} being larger in magnitude than ΔE_{ES}. Indeed for small GaAs dots the difference $(\Delta E_{ES} - \Delta E_{GS})$ can be quite substantial, particularly in the case of 2D dots. This is expected to have some important effect on the optical absorption properties of this quantum dot.

6. Conclusion

In conclusion, we have studied the motion of an electron in a multidimensional symmetric polar semiconductor quantum dot with parabolic confinement in all the spatial directions. We have employed the LLPH variational method to obtain the polaronic corrections to the ground and the first excited state energies of the electron for the entire range of the electron–phonon coupling constant and for arbitrary confinement length. For certain limiting cases, namely in the extended and localized state limits, we have obtained simple closed-form analytical expressions. For arbitrary values of α and l we have obtained results numerically for $N = 2$ and $N = 3$. Comparison of the present ground state results with those obtained from the path-integral method shows that the LLPH results are quite accurate. The LLPH method has however one distinct advantage in that it could be applied to the first excited state, which is one of the main aims of the present paper. We have also calculated the number of phonons in the polaron cloud, the size of the polaron and polarization potential in the polaron ground state. We find that the polaronic effects are more pronounced in a 2D dot than in a 3D dot of the same material. For example, we show that the polaronic corrections to the ground and the first excited states of the quantum dot electron are larger in a 2D dot than in a 3D dot and the ground state polarization potential is deeper in a 2D dot than in a 3D dot. We furthermore show that the polaronic corrections to the ground and the first excited state energies of the dot electron increase with decreasing confinement length. This increase is quite slow if the dot size is large but becomes very rapid when l is reduced below a certain value. We also show that as the confinement length decreases the polarization potential becomes more and more deeper and is

thus able to support lower ground and excited state energy level. We have finally applied our theory to the GaAs quantum dot in both two and three dimensions. We show that the ground and the first excited state energy corrections can be considerably large in the GaAs quantum dots if their sizes are of the order of a few nanometres. We observe that below a certain value of the confinement length the difference between the ground and the first excited state energy corrections due to the polaronic interaction is quite substantial, particularly in the case of the 2D dot. This might have some interesting effect on the optical absorption properties of this quantum dot is under investigation.

Acknowledgments

One of the authors (SM) wishes to thank the University Grants Commission, India, for financial support.

References

[1] Reed M A, Bate R T, Bradshaw K, Duncan W M, Frenly W R, Lee J W and Shih H D 1986 *J. Vac. Sci. Technol.* B **4** 358
Kash K, Scherer A, Worlock J M, Craighead H G and Tamargo M C 1986 *Appl. Phys. Lett.* **49** 1043
Cibert J, Petroff P M, Dolan Pearton S J, Gossard A C and English J H 1986 *Appl. Phys. Lett.* **49** 1275
Temkin H, Dolan G J, Panish M B and Chu S N G 1987 *Appl. Phys. Lett.* **50** 413
Reed M A, Randall J N, Aggarwal R G, Matyi R J, Moore T M and Wetsel A E 1988 *Phys. Rev. Lett.* **60** 535
[2] Johnson N F 1995 *J. Phys.: Condens. Matter* **7** 965
[3] Demel T, Heitmann D, Grambow P and Ploog K 1990 *Phys. Rev. Lett.* **64** 788
Lorke A, Kotthaus J P and Ploog K 1990 *Phys. Rev. Lett.* **64** 2559
Liu C T, Nakamura K, Tsui D C, Ismail K, Antoniadis D A and Smith H I 1989 *Appl. Phys. Lett.* **55** 168
Hansen W, Smith T P III, Lee K Y, Brum J A, Knoedler C M, Hong J M and Kern D P 1989 *Phys. Rev. Lett.* **62** 2168
Tewordt M, Law V, Kelly M, Newbury R, Pepper M, Peacock D, Frost J, Ritchie D and Jones G 1990 *J. Phys.: Condens. Matter* **2** 8969
[4] Yip S K 1991 *Phys. Rev.* B **43** 1707
Dellow M W, Beton P H, Langerak C J G M, Foster T J, Main P C, Eaves L, Henini M, Beaumont S P and Wilkinson C D W 1992 *Phys. Rev. Lett.* **68** 1754
Gu S W and Guo K X 1993 *Solid State Commun.* **89** 1023
Zhu K D and Gu S W 1993 *Phys. Lett.* A **172** 296
Sikorski C and Merkt U 1989 *Phys. Rev. Lett.* **62** 2164
Burs L E 1984 *J. Chem. Phys.* **80** 4403
Halonen V, Chakraborty T and Pietilainen P 1992 *Phys. Rev.* B **45** 5980
Bryant G W 1988 *Phys. Rev.* B **37** 8763
Bryant G W 1990 *Phys. Rev.* B **41** 1243
Bryant G W 1987 *Phys. Rev. Lett.* **59** 1140
Merkt U, Huser J and Wagner M 1991 *Phys. Rev.* B **43** 7320
Marzin J Y and Bastard G 1994 *Solid State Commun.* **92** 437
Johnson N F and Payne M C 1991 *Phys. Rev. Lett.* **67** 1157
[5] Schmitt-Rink S, Miller D A B and Chemla D S 1987 *Phys. Rev.* B **35** 8113
Pan J S and Pan B H 1988 *Phys. Status Solidi* b **148** 128
Roussignol P, Ricard D and Flytzanis C 1989 *Phys. Rev. Lett.* **62** 312
Yip S K 1989 *Phys. Rev.* B **40** 3682
Bockelmann U and Bastard G 1990 *Phys. Rev.* B **42** 8947
Klein M C, Hache F, Ricard D and Flytzanis C 1990 *Phys. Rev.* B **42** 11 123
Bawendi M G, Wilson W L, Roghberg L, Carrol P J, Jedju T M, Steigerwald M L and Bous L E 1990 *Phys. Rev. Lett.* **65** 1623
Nomura S and Kobayashi T 1992 *Phys. Rev.* B **45** 1305
[6] Zhu K D and Gu S W 1992 *Phys. Lett.* A **163** 435
Zhu K D and Gu S W 1992 *J. Phys.: Condens. Matter* **4** 1291

Zhu K D and Gu S W 1993 *Phys. Rev.* B **47** 12 941
Zhu K D and Kobayashi T 1994 *Solid State Commun.* **92** 353
Degani M H and Farias G A 1990 *Phys. Rev.* B **42** 11 950
Mukhopadhyay S and Chatterjee A 1995 *Phys. Lett.* A **204** 411
Mukhopadhyay S and Chatterjee A 1996 *J. Phys.: Condens. Matter* **8** 4017
Mukhopadhyay S and Chatterjee A 1997 *Phys. Rev.* B **55** 9279
[7] Mukhopadhyay S and Chatterjee A 1996 *Int. J. Mod. Phys.* B **10** 2781
[8] Sahoo S 1996 *Z. Phys.* B **101** 97
[9] Mitra T K, Chatterjee A and Mukhopadhyay S 1987 *Phys. Rep.* **153** 91
[10] Maksym P A and Chakraborty T 1990 *Phys. Rev. Lett.* **65** 108
Peeters F M 1990 *Phys. Rev.* B **42** 1486
Li Q P, Karrai K, Yip S K, Das Sarma S and Drew H D 1991 *Phys. Rev.* B **43** 5151
Brey L, Johnson N F, Dempsey J and Halperin B I 1990 *Proc. NATO Adv. Res. Workshop on Light Scattering in Semiconductor Structures and Superlattices (Mont Tremblant, 1990)* (New York: Plenum)
Kumar A, Laux S E and Stern F 1990 *Phys. Rev.* B **2** 5166
[11] Peeters F M, Xiaoguang Wu and Devreese J T 1986 *Phys. Rev.* B **33** 3926
[12] Huybrechts W J 1977 *J. Phys. C: Solid State Phys.* **10** 3761
[13] Chatterjee A 1990 *Ann. Phys., NY* **202** 320
[14] Lee T D, Low F and Pines D 1953 *Phys. Rev.* **90** 297
[15] Kartheuser E 1972 *Polaron in Ionic Crystals and Polar Semiconductors* ed J T Devreese (Amsterdam: North-Holland) p 717